

# Fuzzy logic rotor currents control of a DFIG-based wind turbine

Wiam Ayrir<sup>#1</sup>, Ourahou Meriem<sup>#2</sup>, Ali Haddi<sup>#3</sup>

<sup>#</sup>Laboratory of Innovative Technologies (LTI), University of ABDELMALEK ESSAÄDI, (ENSA) Tangier, Morocco

<sup>1</sup>ayrir-ouiam@hotmail.com

**Abstract**— this paper proposes the control of the rotor-side PWM converter of a variable speed doubly fed induction generator based wind turbine using rotor flux oriented vector control based fuzzy logic. Two fuzzy logic controllers were used to control the direct and the quadratic rotor currents as an alternative of the conventional proportional and integral (PI) controller to overcome any disturbance. The system' model is developed in MATLAB/SIMULINK.

**Keywords**—DFIG, wind turbine, TSR, fuzzy logic.

## Nomenclature:

$R_s, R_r$  : Stator and rotor phase resistances  
 $L_s, L_r$  : Stator and rotor phase inductances  
 $M$  : the mutual inductance  
 $p$  : Number of poles pair of the machine  
 $C_m$  : The mechanical torque  
 $f$  : Friction coefficient  
 $J$  : Moment of inertia  
 $\Omega_{tur}$  : The mechanical speed of the turbine.  
 $\Omega_{mec}$  : The generator speed.  
 $C_{aer}$  : The torque applied on the shaft of turbine.  
 $C_g$  : The torque applied on the shaft of the generator.

## I. INTRODUCTION

Wind energy is the fastest growing in terms of installed capacity among all renewable energy sources [1]. The cumulative installed wind power capacity reached 432 GW in 2015 [2]. Furthermore, the contribution of wind power in the world total generation capacity is expected to reach 8% by 2018 [1], to achieve 12% by 2020 [3] and 20% by 2030 [4]. Currently and over the last few years. DFIG based wind turbines have received an increasing attention and dominate the world market due to variable-speed operation with reduced mechanical stress [5], high controllability, smoother grid connection, maximum power extraction and reactive power compensation using back to back power converters of rating near to 25-30% of the generator capacity[6], as well as the controlling flexibility of reactive power. The basic structure of a DFIG wind turbine is shown on Fig 1. Many different structures and control algorithm could be used to control the rotor side converter. One of the most common techniques is by controlling the rotor' currents. This paper presents the modeling and the control of the DFIG equipped with back-to-back converters. A Fuzzy inference system is applied as an alternative of the conventional

proportional and integral controller (PI). The fuzzy logic control has the advantage to be robust and relatively simple to design, since it does not require the knowledge of the exact model [7]. The performance of the fuzzy logic controller is compared with that of the PI controller, and it is shown that the dynamic performance of fuzzy logic controller is better in comparison with the PI controller.

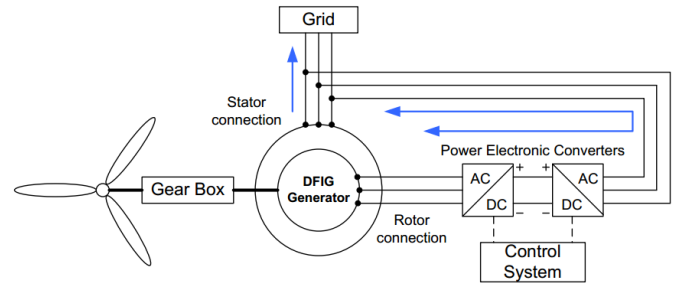


Fig.1: Wind Energy Conversion System with DFIG

## II. WIND TURBINE MODELING

The mechanical power extracted from the wind can be expressed as follow:

$$P_m = 0.5\rho \pi R^2 v^3 C_p(\lambda, \beta) \quad (1)$$

Where  $\rho$  is the air density ( $\text{kg}/\text{m}^3$ ),  $R$  is the blade radius (m),  $v$  is the wind speed,  $C_p$  is the turbine power coefficient, and  $\lambda$  is the tip speed ratio, which is defined by:

$$\lambda = \frac{\Omega_{tur} R}{v} \quad (2)$$

$C_p$  is given by:

$$C_p(\lambda, \beta) = c_1 \left( \frac{c_2}{\lambda_i} - c_3 \beta - c_4 \right) e^{-\frac{c_5}{\lambda_i}} + C_6 \lambda_i \quad (3)$$

With:

$$\frac{1}{\lambda_i} = \frac{1}{\lambda + 0.08\beta} - \frac{0.035}{\beta^3 + 1} \quad (4)$$

The aerodynamic torque is given by:

$$C_{aer} = \frac{1}{2} \cdot \rho \cdot S \cdot C_p \cdot v^3 \cdot \frac{1}{\Omega_{tur}} \quad (5)$$

The Gearbox model:

$$C_m = \frac{C_{aer}}{G} \quad (6)$$

$$\Omega_{mec} = \Omega_{tur} \cdot G \quad (7)$$

The dynamic equation of the wind turbine is given by:

$$\left(\frac{J_t}{G^2} + J_m\right) \frac{d\Omega_m}{dt} + f \cdot \Omega_m = C_m - C_{em} \quad (8)$$

Where  $\frac{J_t}{G^2} + J_m$  is the system total inertia,  $C_m$  is the torque developed by the turbine.  $C_{em}$  is the torque due to load, which in this case is the electromagnetic torque of the generator.

### III. SPEED CONTROL : TIP SPEED RATIO BASED MPPT METHOD:

The objective of this control method is to keep  $\lambda$  at its optimum value  $\lambda_{opt}$ . At this value, the power coefficient is equal to its maximum value.

The pitch angle ( $\beta$ ) is set to zero due to the assumption of fixed pitch wind turbine[8].

So according to equation (2):

$$\Omega_{tur} = \frac{\lambda v}{R} \quad (9)$$

Therefore, if the wind speed changes, the referential speed is given by:

$$\Omega_{tur.ref} = \frac{\lambda_{opt} v}{R} \quad (10)$$

The block diagram of this control method is shown in the following figure [9]:

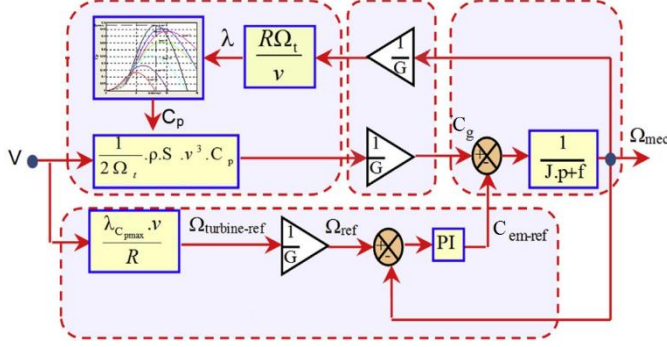


Fig.2: Diagram block of the TSR based MPPT

### IV. MODELLING OF THE DFIG

The general model for the doubly fed induction generator is resumed as follows:

$$\begin{aligned} V_{ds} &= R_s I_{ds} + \frac{d}{dt} \Psi_{ds} - \omega_s \Psi_{qs} \\ V_{qs} &= R_s I_{qs} + \frac{d}{dt} \Psi_{qs} + \omega_s \Psi_{ds} \\ V_{dr} &= R_r I_{dr} + \frac{d}{dt} \Psi_{dr} - \omega_r \Psi_{qr} \\ V_{qr} &= R_r I_{qr} + \frac{d}{dt} \Psi_{qr} + \omega_r \Psi_{dr} \end{aligned} \quad (11)$$

The flux linkage equations:

$$\begin{aligned} \Psi_{ds} &= L_s I_{ds} + M I_{dr} \\ \Psi_{qs} &= L_s I_{qs} + M I_{qr} \\ \Psi_{dr} &= L_r I_{dr} + M I_{ds} \\ \Psi_{qr} &= L_r I_{qr} + M I_{qs} \end{aligned} \quad (12)$$

The electromagnetic torque generated by the DFIG is given by:

$$C_{em} = \frac{pM}{L_s} (\Psi_{ds} I_{qr} - \Psi_{qs} I_{dr}) \quad (13)$$

### V. VECTOR CONTROL STRATEGY:

The rotor flux is set aligned with the d axis. So we can write:

$$\Psi_{qr=0} \quad (14)$$

The electromagnetic torque:

$$C_{em} = -p \Psi_{dr} I_{qr} \quad (15)$$

We define the intermediate rotor voltages as [10]:

$$V_{1dr} = V_{dr} - \frac{M}{L_s} V_{ds} \quad (16)$$

$$V_{1qr} = V_{qr} - \frac{M}{L_s} V_{qs} \quad (17)$$

So we get :

$$V_{1dr} = R_r I_{qr} + L_r \sigma \frac{dI_{dr}}{dt} - \frac{MR_s}{L_s} I_{ds} - \omega_r \Psi_{qr} + \frac{M}{L_s} \omega_s \Psi_{qs} \quad (18)$$

$$V_{1qr} = R_r I_{qr} + L_r \sigma \frac{dI_{qr}}{dt} - \frac{MR_s}{L_s} I_{qs} + \omega_r \Psi_{dr} - \frac{M}{L_s} \omega_s \Psi_{ds} \quad (19)$$

With: 
$$\sigma = 1 - \frac{M^2}{L_s L_r} \quad (20)$$

Equations (18) and (19) could be written as:

$$V_{1dr} = V_{dr1} + V_{dr11} \quad (21)$$

$$V_{1qr} = V_{qr1} + V_{qr11} \quad (22)$$

With:

$$V_{dr1} = R_r I_{dr} + L_r \sigma \frac{dI_{dr}}{dt} \quad (23)$$

$$V_{qr1} = R_r I_{qr} + L_r \sigma \frac{dI_{qr}}{dt} \quad (24)$$

$V_{dr11}$  and  $V_{qr11}$  are the coupling terms. They are eliminated using the classical compensation, which consists of regulating the rotor currents by neglecting these terms, then adding them to the output of the current correctors to obtain the referential rotor voltages. The structure of the current controller is shown below in fig 5. The components of the rotor current ( $I_{dr}$ ,  $I_{qr}$ ) have the same control loop.

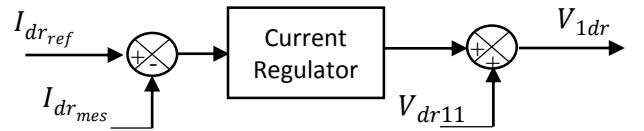


Fig 3: rotor current regulator

In the classical vector control, the rotor currents are controlled using Proportional-Integral correctors.

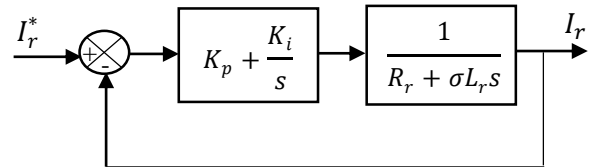


Fig 4: the scheme of the rotor current corrector

The opened-loop transfer function is given by:

$$G(s) = \left(K_p + \frac{K_i}{s}\right) \frac{1}{R_r + \sigma L_r s} \quad (25)$$

Using the poles compensation method:

$$\frac{K_i}{K_p} = \frac{R_r}{\sigma L_r} \quad (26)$$

We get:

$$G(s) = \frac{K_p}{\sigma L_r} \frac{1}{s} \quad (27)$$

The closed-loop transfer function is given by:

$$H(s) = \frac{K_p}{\sigma L_r} \frac{1}{s + \frac{K_p}{\sigma L_r}} \quad (28)$$

The closed-loop transfer function could be written as a first order transfer function:

$$H(s) = \frac{1}{1 + s\tau_c} \quad (29)$$

With:

$$\tau_c = \frac{\sigma L_r}{k_p} \quad (30)$$

$\tau_c$ : The response time.

Finally, we get:

$$K_p = \frac{\sigma L_r}{\tau_c} \quad \text{and} \quad K_i = \frac{R_r}{\tau_c} \quad (31)$$

## VI. FUZZY LOGIC ROTOR CURRENTS CONTROLLER

The dynamic mathematical model of DFIG is a nonlinear, complex and multivariable time-varying system. Fuzzy logic control has the capability to control nonlinear, uncertain and adaptive systems, which gives a strong robust performance for parameters variation [11]. So in order to design a fuzzy controller, the following steps must be performed:

- **Fuzzification:** The process of decomposing a system input and/or output into one or more fuzzy sets using fuzzy linguistic variables and membership functions.
- **Fuzzy rules:** It consists of the development of suitable rules set.
- **Defuzzification:** It consists of the conversion of a fuzzy quantity to a precise quantity.

For the proposed control, the rotor current's error  $e(t)$  and the change of the error  $de(t)$  are used as inputs. The rotor voltage is used as output. The controller observes the pattern of the error signal and its derivative of the direct and quadratic rotor currents components control loops and correspondingly updates the output  $U$  so that the rotor current matches its reference. These two signals are normalized through their respective scaling factors  $K_e$  and  $K_{de}$ . The output control signal  $U$  is derived by multiplying the  $du/dt$  by the output scale factor  $K_{du}$ , and then integrated to generate the command signal.

The simplified block diagram of the fuzzy logic controller is presented on fig 7.

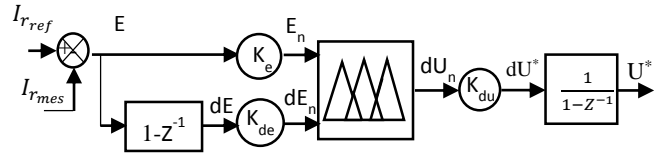


Fig 5: the proposed fuzzy current controller

### A. Membership functions:

A simple Gaussian curve membership function is used for inputs (see fig 6) and a triangular membership function is used for the output (see fig 7).

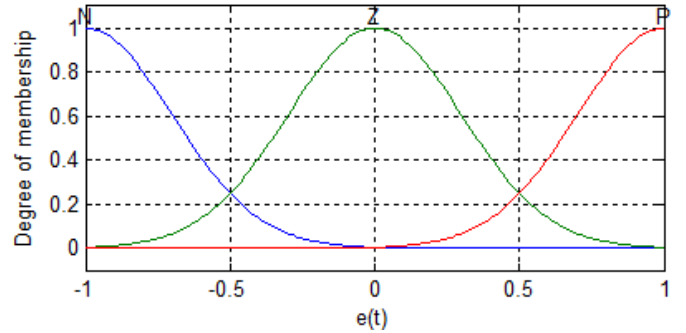


Fig 6: The membership functions for the inputs

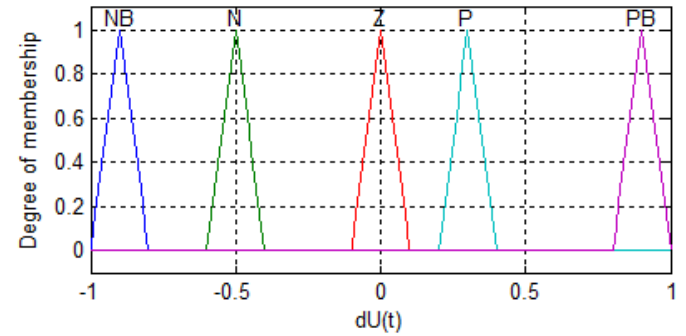


Fig 7: The membership functions for the output

### B. The fuzzy rules:

TABLE I:  
RULE BASES OF THE FUZZY CONTROLLER

		e(t)		
		P	EZ	N
de(t)	P	PB	N	NB
	EZ	PB	EZ	NB
	N	PB	P	NB

### C. Defuzzification

To obtain the output of the FLC, the defuzzification used is based on the center of gravity method.

## VII. SIMULATIONS AND RESULTS ANALYSIS

The simulation of WECS based on DFIG has been performed for two wind speed profiles. The detail parameters used for the simulation:  $c_1=0.5176$ ;  $c_2=116$ ;  $c_3=0.4$ ;  $c_4=5$ ;  $c_5=21$ ;  $c_6=0.0068$ ;  $\lambda_{opt}=8.1$ ;  $C_{p_{max}}=0.5$ ;  $V_{dc}= 500 \text{ V}$ ;  $R_s=1.75 \ \Omega$ ;  $R_r=1.68 \ \Omega$ ;  $L_s=0.295 \text{ H}$ ;  $L_r=0.104 \text{ H}$ ;  $M=0.165 \text{ H}$ ;  $J=0.01 \text{ Kg.m}^2$ ;  $f=0.0027 \text{ Nm.s.rad}^{-1}$ ;  $p=2$ .

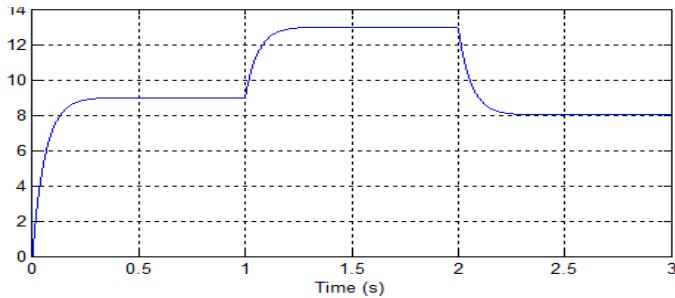


Fig 8: the wind speed profile

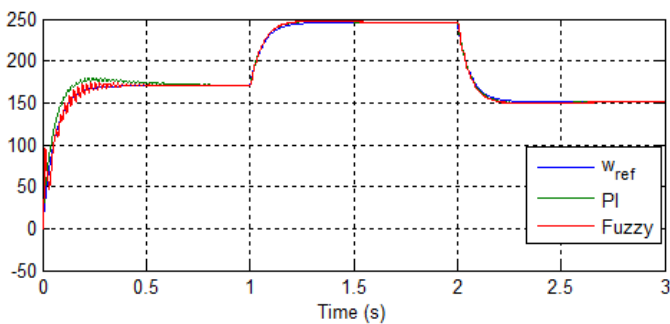


Fig 9: the mechanical speed

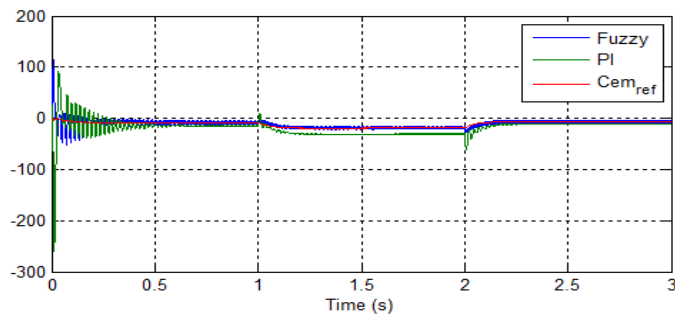


Fig 10: The electromagnetic torque

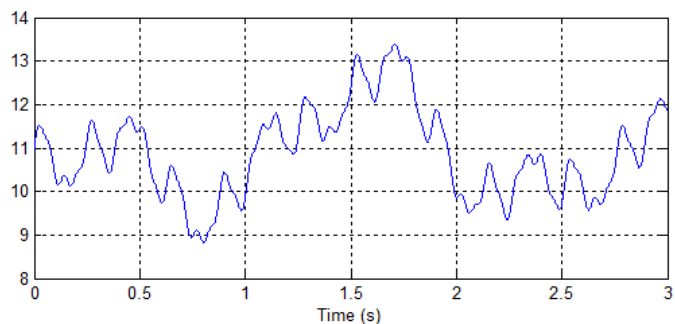


Fig 11: the wind speed profile

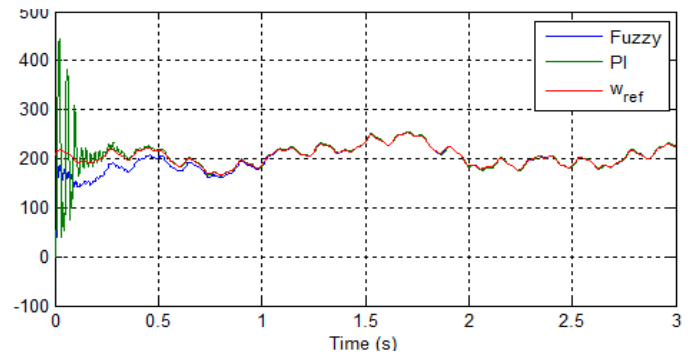


Fig 12: the mechanical speed

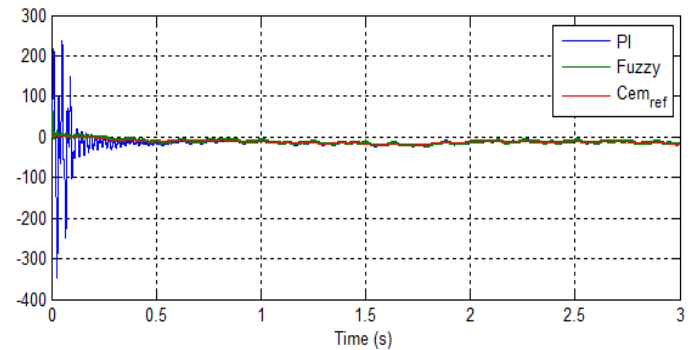


Fig 13: the electromagnetic torque.

According to fig 9, the fuzzy controller presents a faster response time than the PI controller. While for the electromagnetic torque shown in fig 10, it is clearly seen that the PI controller exhibits a relatively long transient period and presents a significant overshoot.

For the second wind speed profile, for the mechanical speed shown in fig 12: the response time of the PI controller is better than the fuzzy one, but in the same time, a significant overshoot is seen. In addition, for the electromagnetic torque (fig 13): the fuzzy controller presents a faster response time and a faster transient response in comparison with the PI controller.

The results obtained show that the rotor flux oriented vector control gives good performances for both the conventional PI controller and the fuzzy logic controller. The mechanical speed and the torque track perfectly their references for both wind speed profiles. Moreover, the fuzzy controller has better performances than the PI controller. Which shows the perfect adaptation of the fuzzy logic control to the rotor flux oriented vector control.

## VIII. CONCLUSIONS

The rotor flux oriented vector control applied to a variable speed DFIG based wind turbine was presented in this paper. A comparative study was made between the PI controller and the fuzzy controller. The fuzzy logic control has the advantage to be robust and relatively simple to design since it does not require the knowledge of the exact model. Moreover, it presents a better performance in tracking the references compared to the conventional PI.

## REFERENCES

- [1] P. Tchakoua, R. Wamkeue, M. Ouhrouche, F. Slaoui-hasnaoui, T. A. Tameghe, and G. Ekemb, "Wind Turbine Condition Monitoring: State-of-the-Art Review, New Trends, and Future Challenges," pp. 2595–2630, 2014.
- [2] "Global wind energy council, GLOBAL WIND REPORT ANNUAL MARKET UPDATE." [Online]. Available: <http://www.gwec.net/>.
- [3] Y. Amirat *et al.*, "A brief status on condition monitoring and fault diagnosis in wind energy conversion systems A Brief Status on Condition Monitoring and Fault Diagnosis in Wind Energy Conversion Systems," 2010.
- [4] F. Iov, A. D. Hansen, P. Sørensen, and N. A. Cutululis, *Mapping of grid faults and grid codes*, vol. 1617, no. July. 2007.
- [5] S. Sharma, "Simulation and Analysis of DFIG System with Wind Turbine Implementing Fuzzy Logic Controller," no. Iconce, pp. 154–159, 2014.
- [6] B. D. Gidwani, "Wind Energy Conversion System using Back to Back Power Electronic Interface with DFIG 2 Modeling of Wind Turbine 3 WECS using DFIG with Back to Back Converters," no. 3, pp. 330–334.
- [7] P. Thirumuraugan and R. Preethi, "Closed Loop Control of Multilevel Inverter Using SVPWM for Grid Connected Photovoltaic System," vol. 2, no. 4, pp. 1561–1572, 2013.
- [8] C. Balasundar, S. Sudharshanan, and R. Elakkiyavendan, "Design of an Optimal Tip Speed Ratio Control MPPT Algorithm for Standalone WECS," vol. 3, no. V, 2015.
- [9] I. Hamzaoui, F. Bouchafaa, and A. Talha, "DPC and DTC control strategies for wind turbine of DFIG with flywheel energy storage system dedicated to improving the quality of energy," vol. 5176.
- [10] K. E. L. Khil, "Commande Vectorielle d' une Machine Asynchrone Doublement Alimentée," 2006.
- [11] A. Dida and D. B. E. N. Attous, "Doubly-fed induction generator drive based WECS using fuzzy logic controller," vol. 9, no. 3, pp. 272–281, 2015.